



Cite this: DOI: 10.1039/c6tb00870d

## Structure–activity relationship studies of symmetrical cationic bolasomes as non-viral gene vectors†

Zheng Huang, Yi-Mei Zhang, Qian Cheng, Ji Zhang,\* Yan-Hong Liu, Bing Wang and Xiao-Qi Yu\*

Compared to traditional cationic lipids, bola-type lipids have received much less attention despite their advantages including the ability to form more stable and regular-shaped liposomes. In this report, a series of novel symmetric cationic bolalipids based on lysine or cyclen headgroups were designed and synthesized. Structure–activity relationships including the effect of the hydrophobic chain length and cationic headgroup on liposome formation, DNA binding, the physical property of bolasomes, and gene transfection were systematically studied. Results reveal that an appropriate hydrophobic chain length is essential to form nano-sized bolasomes with good DNA binding and condensation ability. MTS-based cell viability assays showed low cytotoxicity of these bolasome/DNA complexes. **Lys-14-10**, which has a 36-atom-length hydrophobic chain, exhibited the best transfection efficiency in the two cell lines. Flow cytometry and confocal laser microscopy assays reveal that the bolaplexes formed from bolalipids with such a chain might induce the highest cellular uptake. For the cationic headgroup, lysine is more suitable than cyclen for such a bola-type vector. Although the TEs of these bolalipids are still lower than commercially used non-bola lipid lipofectamine 2000, this study may give us some clues for the design of novel bolalipids with higher TE and biocompatibility.

Received 8th April 2016,  
Accepted 15th July 2016

DOI: 10.1039/c6tb00870d

www.rsc.org/MaterialsB

## Introduction

Over the past decades, profiting from the prosperity and development of gene delivery vectors, gene therapy has made significant progress as a potential method for treating many acquired diseases and genetic disorders such as AIDS, cystic fibrosis and Parkinson's disease.<sup>1–3</sup> Meanwhile, these vectors can also load different kinds of therapeutic cargos, which provide an alternative method to traditional chemotherapy used in treating cancers.<sup>4–6</sup> The gene vectors can effectively protect its cargos (nucleic acids) from degradation by nuclease and deliver them to the interior of the target cells.<sup>7</sup> Broadly speaking, the vectors for gene delivery are mainly classified into two categories: viral and non-viral (or synthetic) vectors.<sup>8</sup> Although viral vectors, including retroviruses and adenoviruses,<sup>9,10</sup> are efficient in delivering nucleic acids to numerous cell lines, they have several drawbacks such as immunogenicity, inflammatory reactions and problems with respect to scale-up procedures.<sup>1,11,12</sup> These limitations

tremendously restricted their applications in clinical trials.<sup>13</sup> Consequently, alternative delivery vectors have been proposed based on synthetic materials such as cationic lipids,<sup>14,15</sup> polymers,<sup>16–19</sup> dendrimers,<sup>20,21</sup> and peptides.<sup>22</sup>

Amongst the non-viral delivery systems reported in the literature, cationic lipids, as the most explored type of non-viral vectors, have shown great potential in gene delivery because of their lower immunogenic nature, ability to deliver large pieces of nucleic acids and ease of handling and preparation.<sup>23</sup> The vast majority of traditional lipids researched so far are “monopolar” amphiphiles. The chemical structure of these molecules generally comprises just one polar headgroup, which is attached to hydrophobic tails *via* a linker. In comparison, bipolar amphiphiles, which are also called bolalipids, are reported much less.<sup>24</sup> In detail, bolalipids are composed of one or two hydrophobic chains that are covalently linked at both ends to hydrophilic head groups.<sup>25–27</sup> Bolalipids can generate monolayer lipid membranes (MLMs) in solution, which may form spherical nanoparticles under ultrasonication.<sup>26,28</sup> This type of molecular architecture mainly presents in archaeobacterial membranes and may ensure their survival in extreme environments (*e.g.* high temperature and low pH) due to its exceptional stability compared to the traditional double-layered membranes.<sup>24,29,30</sup> These amphiphilic compounds have been used in numerous applications including gene delivery.

Key Laboratory of Green Chemistry & Technology (Ministry of Education),  
College of Chemistry, Sichuan University, Chengdu 610064, P. R. China.  
E-mail: xqyu@scu.edu.cn, jzhang@scu.edu.cn; Fax: +86-28-85415886

† Electronic supplementary information (ESI) available: Supplemental figures and compounds characterization. See DOI: 10.1039/c6tb00870d

It was reported that the bolosomes, which were formed from bolalipids with the presence of a helper fusogenic lipid such as 1,2-dioleoyl-*sn*-glycero-3-phosphoethanolamine (DOPE), are capable of delivering genes to target cells.<sup>31,32</sup> One of the earliest studies utilizing cationic bolalipids as non-viral gene delivery agents was carried out by Eaton *et al.*<sup>33</sup> Weissig and co-workers also designed and synthesized a series of bolalipids based on dequalinium (DQAsomes) for mitochondria-targeting gene delivery.<sup>34,35</sup> From then on, a variety of cell targeting bolalipids designed for gene delivery have been reported.<sup>36–41</sup> Most recently, Shapiro *et al.* synthesized two bolalipid compounds with positively charged headgroups from jojoba oil, and they studied the aggregate structures using molecular dynamics (MD) simulations and utilized them as carriers for siRNA delivery.<sup>42</sup>

Although there are some reports about bolalipid-based non-viral gene delivery vectors, the transfection efficiency (TE) is not very satisfying and the structure–activity relationship of bola-type vectors needs further study. Herein we designed and synthesized a series of symmetric cationic bolalipids. The hydrophobic skeleton was constructed by the condensation of saturated aliphatic dicarboxylic acids and  $\alpha,\omega$ -diols. Then hydrophilic cationic headgroups (cyclen or lysine) were linked on the two ends by esterification to gain the final products. Bolosomes were prepared by using these molecules with DOPE. Their interaction with DNA and gene delivery abilities were systematically studied, and the structure–activity relationship (SAR) was discussed. This work may afford new strategy for the construction of bola-type lipids and may give some clues for further improvements of bola-type gene vectors.

## Experimental section

### Materials and methods

All of the common chemicals and reagents were obtained commercially and were used as received. Anhydrous chloroform and dichloromethane were dried and purified under nitrogen by using standard methods and were distilled immediately before use. [4,7,10-Tris(*tert*-butoxycarbonyl)-1,4,7,10-tetraaza-cyclododecan-1-yl] acetic acid (3Boc-cyclen acetic acid) and 2Boc-lysine were prepared according to the literature.<sup>25,43</sup> 1,4,7,10-Tetraazacyclododecanes (cyclen) was purchased from Quzhou Synpartner Pharmaceutical Technology Co., Ltd. 1,2-Dioleoyl-*sn*-glycero-3-phosphoethanolamine (DOPE) was purchased from Avanti Polar Lipids, Inc. pUC19 DNA was purchased from TIANTAI (Chengdu, China). MicroBCA protein assay kit was obtained from Pierce (Rockford, IL, USA). Luciferase assay kit and MTS (3-(4,5-dimethylthiazol-2-yl)-5-(3-carboxymethoxyphenyl)-2-(4-sulfophenyl)-2H tetrazolium, inner salt) were purchased from Promega (Madison, WI, USA). Endotoxin-free plasmid purification kit was purchased from TIANGEN (Beijing, China). The plasmids used in the study were pGL-3 (Promega, Madison, WI, USA) coding for luciferase and pEGFP-N1 (Clontech, Palo Alto, CA, USA) coding for EGFP. The Dulbecco's modified Eagle's medium (DMEM), fetal bovine serum (FBS) and Lipofectamine<sup>®</sup> 2000 were purchased from Invitrogen Corp. The <sup>1</sup>H NMR and <sup>13</sup>C NMR spectra were

measured on a Bruker AM400 NMR spectrometer. Proton Chemical shifts of NMR spectra were given in ppm relative to internal reference TMS (1H, 0.00 ppm). HRMS spectral data was recorded on a Bruker Daltonics Bio TOF mass spectrometer.

The ethidium bromide replacement assay, dynamic light scattering (DLS) experiments, transmission electron microscopy (TEM), amplification and purification of plasmid DNA, cell culture, these procedures were performed according to our reported literature.<sup>16,44</sup>

### Synthesis of the bolalipids

**Preparation of compound 2.** Compound 1 (1,6-hexanediol, 1,8-octanediol, 1,10-decanediol or 1,12-dodecanediol, 20 mmol) and imidazole (1.28 g, 20 mmol) were dissolved in dry dichloromethane; a solution of *tert*-butyldimethylsilyl chloride (TBS-Cl, 2.40 g, 16 mmol) in anhydrous dichloromethane (120 mL) was added dropwise under an ice bath. The obtained mixture was then stirred at room temperature overnight. After dilution with Et<sub>2</sub>O (120 mL), the solution was washed with water (3 × 80 mL), dried over anhydrous Na<sub>2</sub>SO<sub>4</sub>, filtered and evaporated under reduced pressure. The residue was purified by silica gel column chromatography (PE : EA = 4 : 1, v/v) to give the product 2 as a colorless liquid.

**Preparation of compound 4.** Saturated aliphatic dicarboxylic acids (adipic acid, suberic acid, sebacic acid, dodecanedioic acid or tetradecanedioic acid, 4.5 mmol) were activated in the presence of dicyclohexylcarbodiimide (DCC, 1.86 g, 9.0 mmol) and *N,N*-dimethylaminopyridine (DMAP, 0.11 g, 1.8 mmol) in 50 mL anhydrous CH<sub>2</sub>Cl<sub>2</sub> in an ice-salt-bath at 0 °C for 30 min. Then product 2 (9.0 mmol) was added and the mixture was stirred at room temperature overnight. The DCC condensation mixture was then filtered, and the filtrate was evaporated under reduced pressure, and a little amount of ethyl acetate was added. The mixture was maintained at 0 °C for half an hour and then filtered. The filtrate was evaporated under reduced pressure to give the crude product which was purified by column chromatography over silica gel (PE : EA = 20 : 1, v/v) to yield the precursors of 4.

Subsequently, 10 drops of BF<sub>3</sub>·Et<sub>2</sub>O were added to the anhydrous dichloromethane solution of the previously obtained precursor and stirred at room temperature for 2 h. The mixture was concentrated to afford an oil, which was further purified by column chromatography on silica gel (EA : PE = 4 : 1, v/v) to yield 4 as a colorless liquid or white powder.

**Preparation of compound 6.** Compound 4 (1.0 mmol) was added to the anhydrous dichloromethane solution (60 mL) containing 3Boc-cyclen acetic acid (1.12 g, 2.2 mmol) or 2Boc-lysine (760.4 mg, 2.2 mmol), DCC (454.0 mg, 2.2 mmol) and DMAP (24.3 mg, 0.2 mmol) in an ice-salt-bath at 0 °C for 1 h and then stirred at room temperature overnight. The DCC condensation mixture was then filtered, and the filtrate was evaporated under reduced pressure, and a little amount of ethyl acetate was added. The mixture was maintained at 0 °C for half an hour and filtered. The filtrate was evaporated under reduced pressure to give the crude products which were purified by column chromatography over silica gel (PE : EA = 1 : 1, v/v) to yield a white solid 6.

**Preparation of bolalipids 7.** Compound **6** (0.5 mmol) was suspended in anhydrous dichloromethane (5 mL), and then, a solution of trifluoroacetic acid (5 mL) in anhydrous dichloromethane (5 mL) was added dropwise under an ice bath. And then, the obtained mixture was stirred at room temperature for 6 h. After the solvent and trifluoroacetic acid were removed, the bola-like lipids **7** were directly obtained as a colourless liquid by treating the residues with anhydrous ethyl ether twice.

The analysis data of the above compounds are listed in the ESI.†

### Formation of bolasomes and bolaplexes

Bolalipid **7** (0.0025 mmol) or its mixture with DOPE in the desired mole ratio was dissolved in anhydrous chloroform (2.5 mL) in autoclaved glass vials. Thin films were made by slowly rotary-evaporating the solvent at room temperature. The last trace of organic solvent was removed by keeping these films under vacuum over 8 h. The dried films and 2.5 mL of Tris-HCl buffer (10 mM, pH 7.4) were preheated to 70 °C, and then the buffer was added to the films resulting in a final bola concentration of 1.0 mM. The mixtures were vortexed vigorously until the films were completely resuspended. Sonication of these suspensions for 5 min in a bath sonicator at 0 °C afforded the corresponding cationic bolasomes, which were then stored at 4 °C.

To prepare the bolaplexes, various amounts of bolasomes were mixed with a constant amount of DNA by pipetting thoroughly at various N/P ratios, and the mixture was incubated for 30 min at room temperature. The theoretical N/P ratio represents the charge ratio of cationic bolalipids to nucleotide base (in mole) and was calculated by considering an average nucleotide mass of 309.

### Gel retardation assay

To determine the formation of the bola/pDNA complex (bolaplexes), bolaplexes of various N/P ratios ranging from 0 to 8 were prepared as described above. A constant amount of 0.125 µg of DNA was used here; 15 µL of each bolaplex solution was electrophoresed on a 1% (W V<sup>-1</sup>) agarose gel containing Gel-Red and Tris-aceate (TAE) running buffer at 135 V for 30 min. DNA was visualized with a UV lamp using a BioRad Universal Hood II.

### Determination of the critical micelle concentration

The critical micelle concentration (CMC) was determined using pyrene as a fluorescence probe. The block copolymer concentration varied from  $1.0 \times 10^{-6}$  mg mL<sup>-1</sup> to 1 mg mL<sup>-1</sup>, and the pyrene concentration was fixed at  $6.0 \times 10^{-7}$  M. The fluorescence spectra were recorded using a HITACHI F-7000 Fluorescence Spectrophotometer. Both the emission and excitation slit widths were 5 nm. The samples were excited at 335 nm and the emission spectra were recorded from 350 to 500 nm. The emission fluorescence values,  $I_{373}$  and  $I_{383}$  at 373 nm and 383 nm, respectively, were used for the subsequent calculations. The CMC was determined from the plots of the  $I_{383}/I_{373}$  ratio *versus* the logarithm of the polymer concentration using the intersection of the linear regression lines as the CMC value.

### Cytotoxicity assays

Toxicities of bolaplexes toward HEK 293 cells and HeLa cells were determined by using the MTS reduction assay following literature procedures. About  $1.0 \times 10^4$  cells per well were seeded into 96-well plates. After 24 h, optimized bola/DOPE formulations were completed with 0.2 µg of pEGFP-N1 DNA at various N/P ratios for 30 min; 100 µL of bolaplexes were added to the cells in the absence of serum. After 4 h of incubation, bolaplex solutions were removed, and 100 µL of media with 10% FBS was added. After 24 h, 20 µL of MTS and 100 µL of PBS were added to each well and the plates were incubated at 37 °C for another 1 h. Then, the absorbance of each sample was measured using an ELISA plate reader (model 680, BioRad) at a wavelength of 490 nm. The cell viability (%) was obtained according to the manufacturer's instruction. Lipoplex prepared from Lipofectamine 2000 was used as a control.

### *In vitro* transfection procedure

In order to obtain about 80% confluent cultures at the time of transfection, 24-well plates were seeded with  $1.0 \times 10^5$  cells per well in 500 µL of antibiotic-free media 24 h before transfection. For the preparation of bolaplexes applied to cells, various amounts of bolasomes and DNA were serially diluted separately in antibiotic-free DMEM culture medium; then, the DNA solutions were added into bolasome solutions and mixed briefly by pipetting up and down several times, after which the mixtures were incubated at room temperature for about 30 min to obtain bolaplexes of desired N/P ratios, the final bolaplex volume was 100 µL, and DNA was used at a concentration of 0.8 µg per well. After 30 min of complexation, the old cell culture medium was removed from the wells, cells were washed once with serum-free DMEM, and the above 100 µL of bolaplexes were added to each well. The plates were then incubated for 4 h at 37 °C in a humidified atmosphere containing 5% CO<sub>2</sub>. At the end of the incubation period, the medium was removed, and 500 µL of fresh DMEM medium containing 10% FBS was added to each well. Plates were further incubated for a period of 24 h before checking the reporter gene expression.

For fluorescent microscopy assays, cells were transfected by complexes containing pEGFP-N1. After a 24 h incubation, the microscopy images were obtained at a magnification of 100 and recorded using Viewfinder Lite (1.0) software. Control transfection was performed in each case using a commercially available transfection reagent Lipofectamine 2000™ based on the standard conditions specified by the manufacturer. After a 24 h transfection of the pEGFP plasmid, cells were lysed and 100 µL of lysate was taken to measure the fluorescence intensity. The excitation wavelength was 485 nm and the emission wavelength was 538 nm. Lipofectamine 2000™ was chosen as a control.

For luciferase assays, cells were transfected by complexes containing pGL-3. For a typical assay in a 24-well plate, 24 h post transfection as described above, the old medium was removed from the wells, and the cells were washed twice with 500 µL of prechilled PBS. According to the luciferase assay kit (promega) manufacture, 100 µL of 1× cell lysis buffer diluted

with PBS was then added to each well, and the cells were lysed for 30 min in a horizontal rocker at room temperature. The cell lysate was transferred completely to Eppendorf tubes and centrifuged (4000 rpm, RT) for 2 min; the supernatant was transferred to Eppendorf tubes and stored in ice. For the assay, 20  $\mu\text{L}$  of this supernatant and 100  $\mu\text{L}$  of the luciferase assay substrate (Promega) were used. The lysate and the substrate were both thawed to RT before performing the assay. The substrate was added to the lysate, and the luciferase activity was measured in a luminometer (Turner designs, 20/20, Promega, USA) in standard single-luminescence mode. The integration time of measurement was 10 000 ms. A delay of 2 s was given before each measurement. The protein concentration in the cell lysate supernatant was estimated in each case with the Lowry protein assay kit (PIERCE, Rockford, IL, USA). A comparison of the transfection efficiencies of the individual bolas was made based on the data for luciferase expressed as relative light units (RLU) per mg of protein. All the experiments were done in triplicates, and the results presented are the average of at least two such independent experiments done on the same days.

### Flow cytometry assay

The cellular uptake of the bolasome/fluorescein labelled-DNA complexes was analyzed by flow cytometry. The label IT Cy5 Labeling Kit was used to label pGL-3 with Cy5 according to the manufacturer's protocol. Briefly, HEK 293 cells were seeded onto 12-well plates ( $2.0 \times 10^5$  cells per well) and allowed to attach and grew for 24 h. Before transfection, the medium was replaced with a serum-free culture medium. Cells were incubated with Cy5 labelled DNA nanoparticles (1.6  $\mu\text{g}$  of DNA per well, optimal N/P ratio of each sample) in media for 4 h at 37  $^\circ\text{C}$ . Subsequently, the cells were washed with  $1 \times$  PBS and harvested with 0.25% trypsin/EDTA and resuspended in  $1 \times$  PBS. Cy5-labelled plasmid DNA uptake was measured in the FL4 channel using the red diode laser (633 nm). Data from 10 000 events were gated using forward and side scatter parameters to exclude cell debris. The flow cytometer (BD Accuri™ C6) was calibrated for each run to obtain a background level of  $\sim 1\%$  for control samples (*i.e.*, untreated cells).

### Confocal laser scanning microscopy (CLSM)

HEK 293 cells were seeded at a density of  $2.5 \times 10^5$  cells per well in a 35 mm confocal dish ( $\Phi = 15$  mm), 24 h prior to transfection. For transfection in the absence of serum, the medium was exchanged with serum-free medium (for transfection with serum, the medium was exchanged with serum-containing medium). Complexes of bolasomes and Cy5-labelled pGL-3 at a given concentration were added to each well. After incubation at 37  $^\circ\text{C}$  for 4 h, cells were rinsed 3 times with PBS (pH 7.4), fixed with 4% paraformaldehyde (dissolved with PBS buffer) for 10 min and nuclear staining was done with DAPI. The CLSM observation was performed using confocal laser scanning microscopy (CLSM, ZEISS LSM 780) at excitation wavelengths of 405 nm for DAPI (blue) and 633 nm for Cy5 (red), respectively. For the endosome escape experiment, after incubation at 37  $^\circ\text{C}$  for different times (4 h, 6 h, 8 h and 12 h), LysoTracker green (1 : 750) was added

into the well for another 30 min incubation at 37  $^\circ\text{C}$ . Then cells were rinsed 3 times with PBS (pH 7.4), fixed with 4% paraformaldehyde (dissolved with PBS buffer) for 10 min, lysosome staining was done with LysoTracker green. The CLSM observation was performed using confocal laser scanning microscopy (CLSM, ZEISS LSM 780) at excitation wavelengths of 504 nm for LysoTracker green (green) and 633 nm for Cy5 (red), respectively.

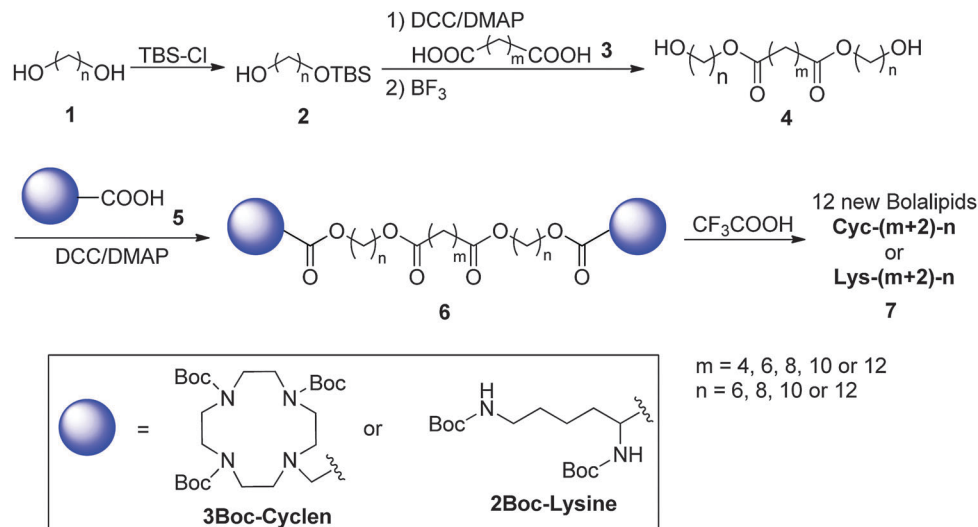
## Results and discussion

### Synthesis of the bolalipids

A series of novel symmetrical cationic bolalipids containing a protonated cyclen or lysine headgroup and various hydrophobic cores were synthesized. The length of the hydrophobic skeleton was adjusted by using dicarboxylic acids and  $\alpha,\omega$ -diols with various chain lengths. The use of cyclen as the hydrophilic head group is based on its unique structural characteristics. Cyclen has four amine groups with different chemical properties such as  $\text{p}K_{\text{a}}$  values. Such diversity makes cyclen a potential candidate for both DNA condensation and pH buffering. Meanwhile, the cyclic backbone that is hard to self-fold can also retain its high DNA binding ability. Our previous studies demonstrated that cyclen-based cationic lipids may act as promising materials for gene delivery.<sup>14,15,43</sup> Lysine has good biocompatibility and excellent DNA binding ability for its two primary amines, and it was also widely used for the cationic headgroup of lipidic vectors.<sup>24,28,45</sup> As shown in Scheme 1, one hydroxyl of  $\alpha,\omega$ -diol was first protected by *tert*-butyldimethylsilyl chloride (TBSCl), then the other hydroxyl was reacted with saturate aliphatic dicarboxylic acid **3** in the presence of dicyclohexylcarbodiimide (DCC) and 4-dimethylaminopyridine (DMAP) to form two ester bonds. Subsequent TBS deprotection by  $\text{BF}_3$  gave the hydrophobic skeleton diol **4** (**Diol**-( $m+2$ )- $n$ ). Compound **4** was coupled with 3Boc-cyclen acetic acid or 2Boc-lysine (**5**) to give the precursor **6**. Then target bolalipids **7** (represented as **Cyc**-( $m+2$ )- $n$  or **Lys**-( $m+2$ )- $n$  based on the headgroup) were obtained by removing the Boc groups with trifluoroacetic acid in anhydrous  $\text{CH}_2\text{Cl}_2$ . The hydrophobic chain length of the bolalipids can be easily calculated as  $(m + 2) + 2n + 2$ , which represent carbon atoms of diacid, carbon atoms of diol, and two oxygens in the middle ester bonds, respectively. For example, **Lys-14-10** has a 36-atom chain between the two cationic headgroups. All novel compounds in each step were purified and their structures were confirmed by  $^1\text{H}$  NMR,  $^{13}\text{C}$  NMR and HRMS. The critical micelle concentrations (CMCs) of two typical bolalipids **Lys-14-10** and **Cyc-14-10** were measured to study their natural aggregation behaviors *via* fluorescence spectrometry using a pyrene probe.<sup>46</sup> Their CMCs were found to be 47.4 and 24.5  $\mu\text{M}$ , respectively (Fig. S1, ESI<sup>†</sup>).

### Formation of bolasomes and their interaction with DNA

In general, cationic lipids usually form liposomes with the presence of a helper fusogenic lipid such as DOPE due to its especial membrane fusion ability.<sup>32</sup> The bolasomes were prepared by using the same strategy with DOPE by the thin film hydration method,<sup>24</sup>



Scheme 1 Synthetic routes of target bolalipids.

and the mole ratio of lipid/DOPE was 1 : 1 according to the best behavior in the transfection experiments (Fig. S2, ESI<sup>†</sup>). For the twelve synthetic bolalipids, it was found that **Cyc-6-6**, **Cyc-8-6**, **Cyc-10-6**, **Cyc-12-6**, **Lys-10-6** and **Lys-12-8** with a relatively shorter chain length could not fuse with DOPE during the hydration process, and a white precipitate was formed. However, the last three bolalipids (**Cyc-12-6**, **Lys-10-6**, **Lys-12-8**) mentioned above could yield a clear solution after 10 min of sonication (Table 1). On the other hand, bolalipids with a longer chain length could form bolosomes well with DOPE, indicating that a special length is necessary for their self-assembly with DOPE (Fig. 1). We chose five typical bolalipids (**Lys-10-6**, **Lys-12-8**, **Lys-14-10**, **Lys-14-12** and **Cyc-14-10**) in the following studies. Gel electrophoresis results reveal that the ability to form bolosomes is essential to DNA binding and condensation. As shown in Fig. 1, most of the materials can effectively bind plasmid DNA and can completely retard DNA migration at the N/P ratio of 4. However, **Lys-10-6**, which has a weaker ability to form a bolosome, showed much lower binding ability, and could not retard DNA even at a higher N/P of 8. For the cationic headgroup, cyclen-derived liposome **Cyc-14-10** seems to have stronger DNA

retardation ability than the lysine-contained ones, and full retardation was observed at N/P of 2. This might be attributed to the more positively charged amino groups in the structure.

To further evaluate the DNA binding ability of the bolosomes, the ethidium bromide (EB) exclusion assay was carried out.<sup>47</sup> EB can produce high fluorescence when intercalating into DNA base pairs. The addition of another agent with higher DNA affinity may expel EB from its intercalation site, leading to fluorescence quenching. The results in Fig. 2 show that the fluorescent intensities caused by EB dramatically decreased in the N/P range of 0–2, indicating the strong binding between the bolosomes and DNA. A further increase of N/P led to only slight fluorescence weakening. More significantly, the fluorescence quenching levels of the five bolosomes were much different. The bolosome formed from **Lys-10-6**, which has the shortest hydrophobic chain, showed the narrowest fluorescence quenching extent, suggesting its weaker DNA binding ability than others. This is consistent with the results obtained in gel electrophoresis. With the increase of the hydrophobic chain, the DNA binding ability of the bolosomes got stronger. Compared to the chain length, the cationic headgroup has less effect on the fluorescence quenching ability, and bolosomes containing lysine or cyclen gave a similar quenching extent (Fig. 2).

The physicochemical characteristics including particle size and zeta-potentials of the prepared bolosomes were measured by dynamic light scattering (DLS). The effect of the bolalipid/DOPE ratio on the properties of bolosomes was firstly studied. It was found that the particle sizes and zeta-potentials dramatically decreased with the participation of DOPE, while a further increase of the DOPE amount didn't cause an obvious change (Fig. S3A and B, ESI<sup>†</sup>). Thus subsequent experiments were performed with the DOPE/bolalipid ratio of 1:1. The average particle sizes of these bolosomes varied from 52 nm to 235 nm. It's clearly shown that the mean size decreased along with the increase of the hydrophobic chain length, also indicating that a special length is important for the formation of nano-sized

Table 1 The solubility of the bolalipid and DOPE mixture in preparation of a bolosome (×: insoluble; √: soluble)

Bolalipids	Hydration	Sonication
<b>Cyc-6-6</b>	×	×
<b>Cyc-8-6</b>	×	×
<b>Cyc-10-6</b>	×	×
<b>Cyc-12-6</b>	×	√
<b>Cyc-12-8</b>	√	√
<b>Cyc-14-6</b>	√	√
<b>Cyc-14-8</b>	√	√
<b>Cyc-14-10</b>	√	√
<b>Lys-10-6</b>	×	√
<b>Lys-12-8</b>	×	√
<b>Lys-14-10</b>	√	√
<b>Lys-14-12</b>	√	√

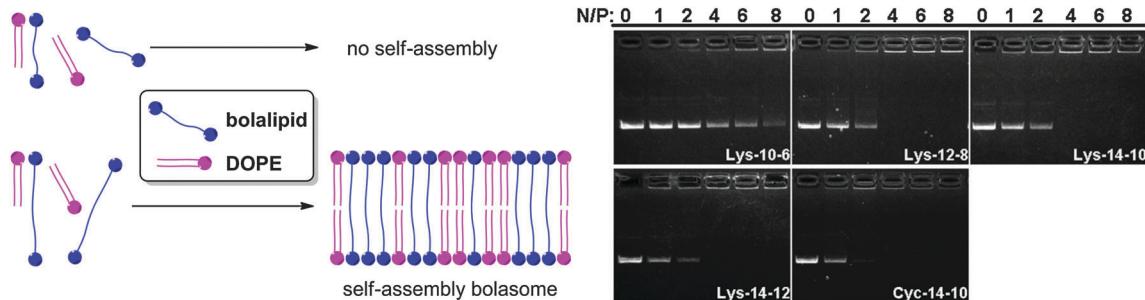


Fig. 1 Left: Schematic illustration for the formation of a bolosome with DOPE; right: electrophoretic gel retardation assays at different N/P ratios. The molar ratio of bolalipid/DOPE was 1 : 1.

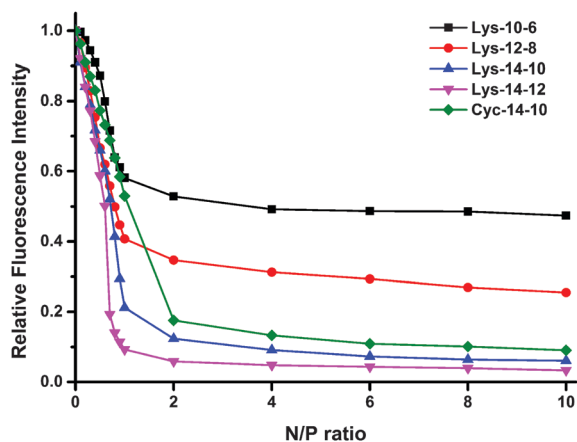


Fig. 2 Fluorescent quenching assay of EB/DNA with the addition of bolosomes. The molar ratio of bolalipid/DOPE was 1 : 1.

particles (Fig. S3C, ESI<sup>†</sup>). In other words, since it was known that liposomes with diameters below 100 nm would have better DNA binding and delivery ability,<sup>48</sup> the chain lengths of **Lys-10-6** and **Lys-12-8** are not long enough to form nanoparticles with the proper size, while **Lys-14-10**, **Lys-14-12** and **Cyc-14-10** could form bolosomes with  $\sim 55$  nm diameters. The zeta potentials of the bolosomes were found in the range of +40–70 mV, and longer

hydrophobic chains resulted in higher potentials (Fig. S3D, ESI<sup>†</sup>). This might also be caused by the smaller liposome particles, which led to increased surface charge density. Although lysine has less amino groups than cyclen, liposomes with a lysine headgroup gave slightly higher potentials than that with cyclen, suggesting that lysine is better protonated in aqueous solution. Then, these physical properties of the bolosome–DNA complexes (bolaplexes) formed from bolalipids 7 were studied. As shown in Fig. 3A, after binding with plasmid DNA, the size of the bolaplex particles increased evidently. Under a lower N/P ratio ( $\leq 4$ ), the particle sizes were irregular due to the incomplete DNA condensation. From a N/P ratio of 6, all bolosomes were able to condense DNA into steady nanosized particles ( $\sim 300$  nm) except **Lys-10-6**, which could not form bolosomes well. Zeta-potentials of the bolaplexes rose along with the increase of the N/P ratio, and the structure–property relationship was similar to the empty bolosomes (Fig. S3D, ESI<sup>†</sup>).

Transmission electron microscopy (TEM) was used to visually study the morphological characteristics of the bolosomes and bolaplexes. The images in Fig. 4 show that lysine-based bolosomes have spherical distribution with the diameters ranging from 40 nm to 100 nm. Interestingly, cyclen-contained bolosome **Cyc-14-10** gave a more homogeneous distribution and much smaller particles (diameter  $\sim 15$  nm), which was supposed to be spherical micelles but not bolosomes. The polyamine ring in

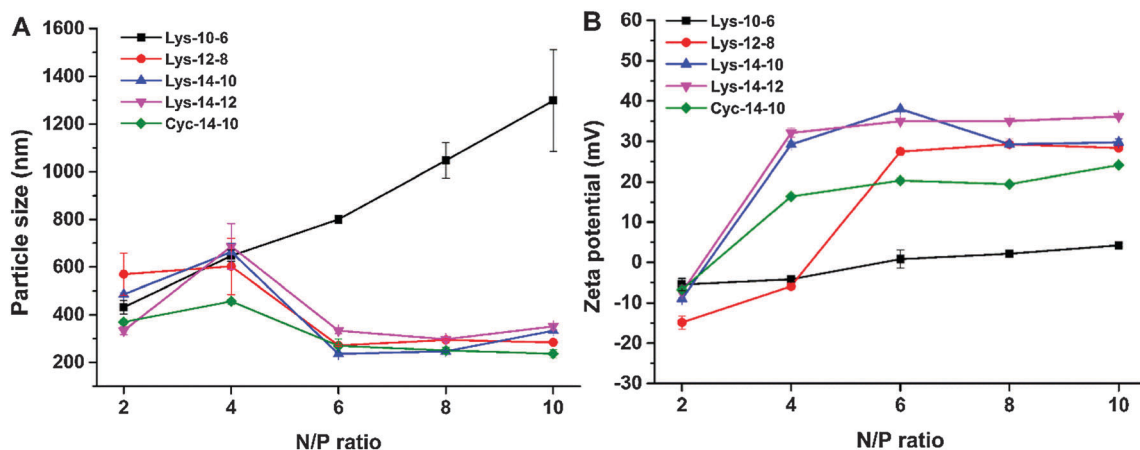


Fig. 3 Mean particle sizes (A) and zeta-potentials (B) of the bolaplexes formed from bolosome and pUC19 DNA under various N/P ratios (DLS at room temperature). Data represent mean  $\pm$  SD ( $n = 3$ ).

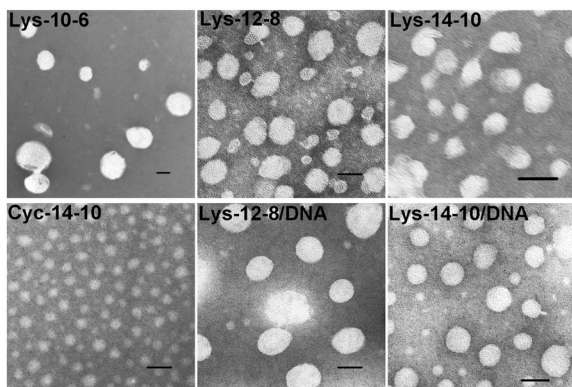


Fig. 4 TEM images of selected bolosomes and bolaplexes. Scale bar: 50 nm.

cyclen has a bigger cross-sectional area than the lysine group, therefore, compared to the bolosomes formed from lysine-derived bolalipids, **Cyc-14-10** might form a micelle structure by bending and folding of the hydrophobic skeleton.<sup>26,42</sup> Furthermore, the last two images show that DNA could also be compacted into spherical nanoparticles with a diameter of 40–60 nm by two lysine-derived bolosomes. The particle sizes determined by TEM were not identical with those obtained by DLS. This might be due to the different experimental conditions: DLS data provide a hydrodynamic size of the particles, which could further aggregate to form larger particles, while in TEM measurements, the particles are stabilized by adsorption on the surface of carbon-coated copper meshes.<sup>49</sup>

### Cytotoxicity

One of the criteria for an ideal non-viral gene delivery vector is to possess a low cytotoxicity profile. Bolosomes have been reported with relatively lower toxicity than traditional cationic liposomes.<sup>50</sup> MTS-based cell viability assays were carried out in HEK 293 and HeLa cells to investigate the cytotoxicity of the bolaplexes at various N/P ratios, and lipid lipofectamine 2000 was used as a positive control. Results shown in Fig. 5 reveal that both cell lines showed higher tolerance against the

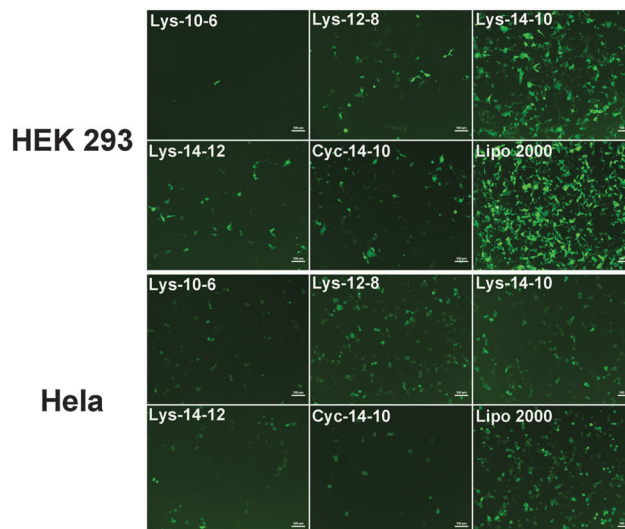


Fig. 6 Fluorescent microscopy images of HEK 293 cells and HeLa cells transfected by bolosomes at the optimal N/P ratio (HEK 293: 12, 10, 6, 6 and 10; HeLa: 12, 6, 4, 4 and 10, respectively). The molar ratio of bola/DOPE was 1:1 and lipofectamine 2000 was used as the control. The cells were observed by fluorescence microscopy after a 24 h transfection. Scale bar: 100  $\mu\text{m}$ .

synthesized materials than the positive control, especially at the N/P ratio used in subsequent transfection assays (<16).

### In vitro gene transfection

The TE of bolaplexes was preliminarily studied by using the green fluorescent protein (GFP) reporter gene. Transfection was mediated by the bolaplexes at various N/P ratios in two cell lines (HEK 293 and HeLa). Fig. 6 shows the eGFP expression in two cell lines at optimal N/P ratios observed by an inverted fluorescent microscope. Although the density of the green fluorescence induced by the bolaplexes was lower than that by lipofectamine 2000, we may find that the TE relied heavily on the chemical structure of the bolalipids. The TE increased with the extension of the hydrophobic chain, and reached the best transfection at **Lys-14-10**. Further elongation of the chain led to

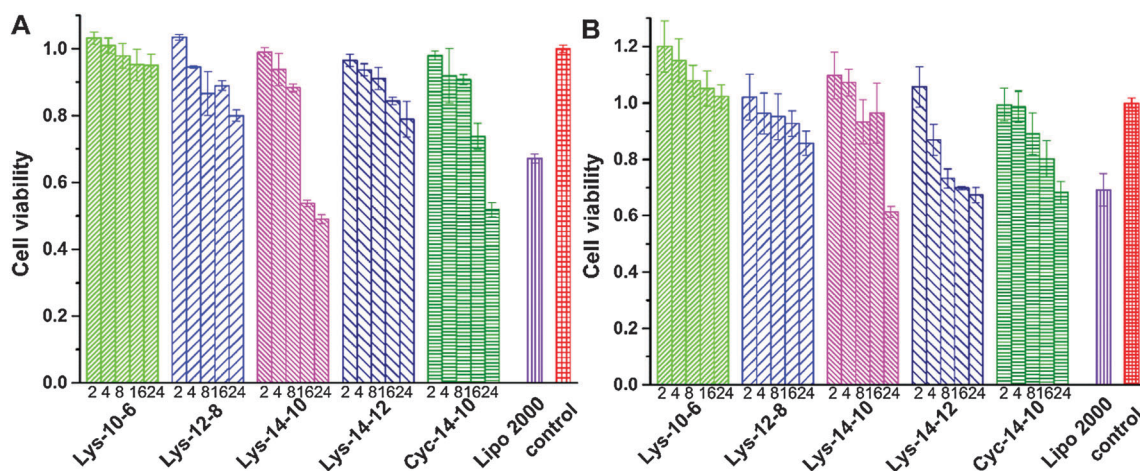


Fig. 5 *In vitro* cytotoxicity of the bolaplexes at various N/P ratios in HEK 293 (A) and HeLa cells (B) for a 24 h incubation. Data represent mean  $\pm$  SD ( $n = 3$ ).

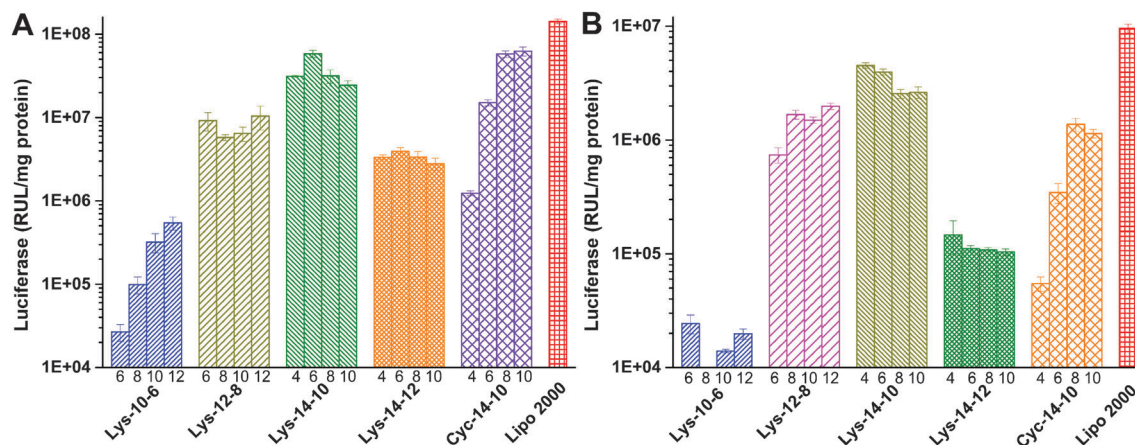


Fig. 7 Luciferase expression in HEK 293 (A) and HeLa (B) cells transfected by bolaplexes at various N/P ratios. Data represent mean  $\pm$  SD ( $n = 3$ ).

a decreased TE (**Lys-14-12**). As for the cationic headgroup, bolaplexes derived from cyclen based bolalipid (**Cyc-14-10**) gave much lower TE than its lysine analog. Moreover, the luciferase reporter gene was also used to quantitatively study the TE of the bolaplexes. As shown in Fig. 7, the results were found to be similar to the GFP assays, and **Lys-14-10** gave the best TE, which was about 50% of lipofectamine 2000. We speculate that **Lys-14-10** has the most proper chain length (36 atoms including 2 oxygens) to form bolosomes with the thickness similar to a cell membrane, leading to better membrane fusion and cellular uptake. Its analog, **Cyc-14-10**, gave comparable TE in HEK 293 cells and much lower TE in HeLa cells. Such results might be attributed to its stronger DNA binding ability (Fig. 1), which would result in more difficult DNA release in the cell. Furthermore, the effect of serum on the TE was also investigated by using three representative bolaplexes (Fig. S4, ESI<sup>†</sup>). Unfortunately, compared to lipofectamine 2000, these bolalipids did not exhibit better serum tolerance, and the TE gave a measurable decrease. However, **Lys-14-10** showed distinctly higher serum resistibility than **Cyc-14-10**, and this might guide us to design novel bolalipids with higher TE and biocompatibility.

The fluorescence-activated cell sorting (FACS) technique was applied for further study of the transfection mechanism mediated by these bolosomes in HEK 293 cells. After a 4 h cell incubation with the bolaplexes at each optimized N/P ratio, the percentage of Cy5-positive cells and the mean fluorescence intensity of Cy5 were calculated and shown in Fig. 8. It was confirmed that a hydrophobic skeleton with the length of “14-10” has superiority for cellular uptake. **Lys-14-10** and **Cyc-14-10** gave significantly higher values in both uptake cell percentage and fluorescence intensity than other bolalipids. However, the values were still lower than the non-bola lipid lipofectamine 2000, and this might contribute to their lower TE in the transfection assays. On the other hand, it was reported that materials with secondary amines showed higher cellular uptake,<sup>51</sup> thus the result that **Cyc-14-10** had a higher cellular uptake than **Lys-14-10** might be reasonable. Nevertheless, **Cyc-14-10** gave lower TE than **Lys-14-10**, also suggesting that good cellular uptake is a necessary but not sufficient condition for high TE. As mentioned above, the stronger DNA binding ability of **Cyc-14-10** may lead to

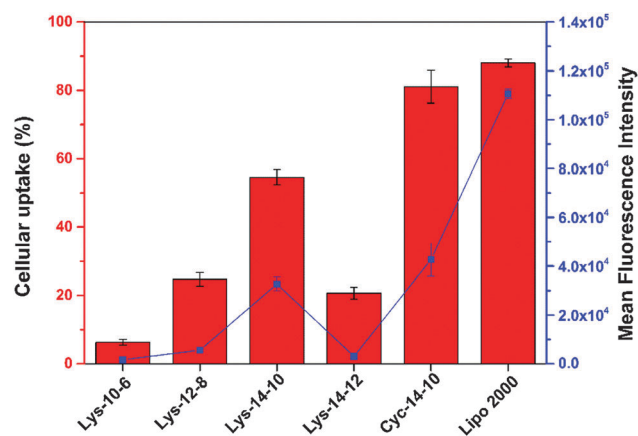


Fig. 8 Cellular uptake (columns, percentage of Cy5-positive cells) and mean fluorescence intensity (dots and lines) of bolaplexes at the optimal N/P ratio in HEK 293 cells quantified by flow cytometry. Lipofectamine 2000 was used as the control. Data represent mean  $\pm$  SD ( $n = 3$ ).

difficult release of DNA and lower transfection. Subsequently, the cellular uptake assays were also carried out using **Lys-14-10** without or with 10% serum in HeLa cells to study the effect of serum. Results in Fig. S5 (ESI<sup>†</sup>) show that the uptake cell percentage and fluorescence intensity were seldom influenced by 10% serum, indicating a comparable serum tolerance to lipofectamine 2000, especially in HeLa cells.

Confocal laser scanning microscopy (CLSM) was also applied to visually examine the internalization and intracellular location of Cy5-labelled DNA transferred by bolaplexes at the optimal N/P ratio in HEK 293 cells. DNA was labelled by Cy5 (red), while the cell nuclei were stained with 4',6-diamidino-2-phenylindole (DAPI, blue). As shown in Fig. 9, after 4 h of incubation with bolaplexes derived from **Lys-14-10** and **Cyc-14-10**, a considerable amount of the fluorescent labelled DNA accumulated in the perinuclear region, while very weak signals were observed for the transfection by the other three bolaplexes. Similarly, the red fluorescence induced by **Cyc-14-10** was slightly stronger than that by **Lys-14-10**, further suggesting a better cellular uptake, which is consistent with the flow

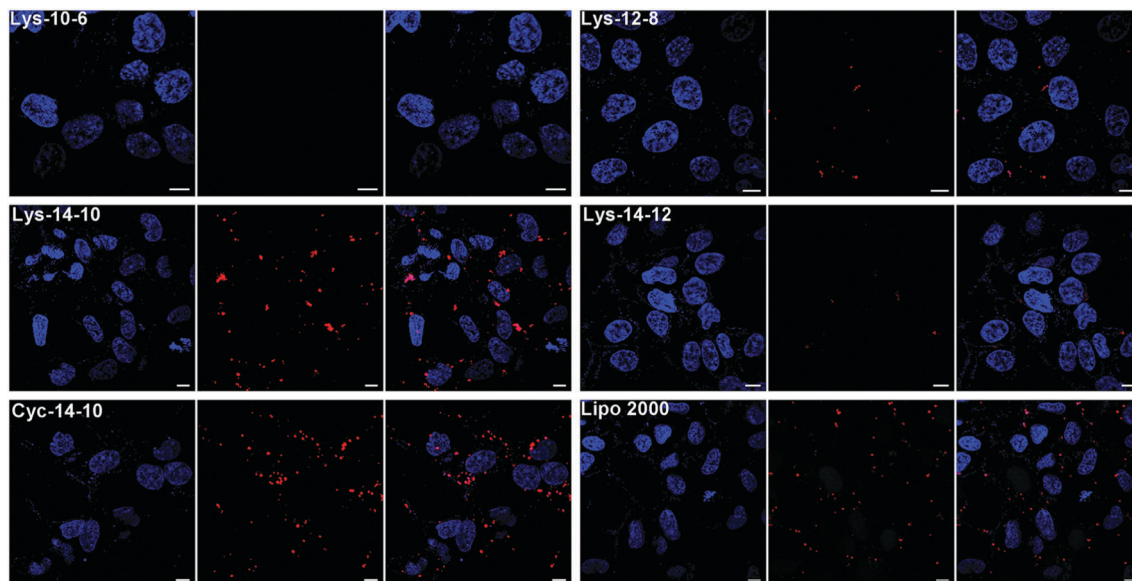


Fig. 9 CLSM images of HEK 293 cells transfected with Cy5-labelled DNA by the bolaplexes at the optimal N/P ratio. For each row, left: cell nuclei stained by DAPI (blue); middle: Cy5-labelled pDNA (red); right: merged image. Scale bar: 10  $\mu$ m.

cytometry results. In addition, the intracellular trafficking of cargo DNA mediated by **Cyc-14-10** and **Lys-14-10** was also studied. Resulting images in Fig. S6 (ESI<sup>†</sup>) demonstrate that DNA (red) could escape well from the endosome/lysosome (green), which is necessary for efficient transfection.

## Conclusions

In summary, a series of novel symmetric cationic bolalipids with various hydrophobic chain lengths were designed and synthesized. Lysine and cyclen were chosen as the cationic headgroup. Structure–activity relationships of these bolalipids in liposome formation, DNA binding, the physical property of the bolasome, and gene transfection were systematically studied. Results reveal that an appropriate hydrophobic chain length is essential to form bolasomes with good DNA binding and condensation ability. Bolalipids with short chains could not condense DNA well, leading to a poor gene transfection efficiency (TE). **Lys-14-10**, which has a 36-atom-length hydrophobic chain, exhibited the best TE in the two cell lines. Flow cytometry and confocal laser microscopy assays reveal that the bolaplexes formed from bolalipids with such a chain might induce the highest cellular uptake. We speculate that the thickness of such bolasomes is close to a cell membrane, thus facilitating the membrane fusion and subsequent endocytosis. Although the TEs of these bolalipids are still lower than commercially used non-bola lipid lipofectamine 2000, this study may give us some clues for the design of novel bolalipids with a higher TE and biocompatibility.

## Acknowledgements

This work was financially supported by the National Program on Key Basic Research Project of China (973 Program, 2012CB720603) and the National Science Foundation of China

(No. 21472131, 21232005). We thank the comprehensive training platform of specialized laboratory, College of Chemistry, Sichuan University for sample analysis.

## References

- 1 I. M. Verma and N. Somia, *Nature*, 1997, **389**, 239–242.
- 2 S. Bhattacharya and A. Bajaj, *Chem. Commun.*, 2009, 4632–4656, DOI: 10.1039/B900666B.
- 3 M. A. Mintzer and E. E. Simanek, *Chem. Rev.*, 2009, **109**, 259–302.
- 4 S. S. Kelkar and T. M. Reineke, *Bioconjugate Chem.*, 2011, **22**, 1879–1903.
- 5 M. Khan, Z. Y. Ong, N. Wiradharma, A. B. E. Attia and Y.-Y. Yang, *Adv. Healthcare Mater.*, 2012, **1**, 373–392.
- 6 H. Wang, Y. Chen, X.-Y. Li and Y. Liu, *Mol. Pharmaceutics*, 2007, **4**, 189–198.
- 7 Z. U. Rehman, I. S. Zuhorn and D. Hoekstra, *J. Controlled Release*, 2013, **166**, 46–56.
- 8 X. Guo and L. Huang, *Acc. Chem. Res.*, 2012, **45**, 971–979.
- 9 Y. Yue and C. Wu, *Biomater. Sci.*, 2013, **1**, 152–170.
- 10 U. Lächelt and E. Wagner, *Chem. Rev.*, 2015, **115**, 11043–11078.
- 11 N. Cartier, S. Hacein-Bey-Abina, C. C. Bartholomae, G. Veres, M. Schmidt, I. Kutschera, M. Vidaud, U. Abel, L. Dal-Cortivo, L. Caccavelli, N. Mahlaoui, V. Kiermer, D. Mittelstaedt, C. Bellesme, N. Lahlou, F. Lefrère, S. Blanche, M. Audit, E. Payen, P. Leboulch, B. l'Homme, P. Bougnères, C. Von Kalle, A. Fischer, M. Cavazzana-Calvo and P. Aubourg, *Science*, 2009, **326**, 818–823.
- 12 K. Braeckmans, K. Buyens, B. Naeye, D. Vercauteren, H. Deschout, K. Raemdonck, K. Remaut, N. N. Sanders, J. Demeester and S. C. De Smedt, *J. Controlled Release*, 2010, **148**, 69–74.

- 13 S. Kang, K. Lu, J. Leelawattanachai, X. Hu, S. Park, T. Park, I. M. Min and M. M. Jin, *Gene Ther.*, 2013, **20**, 1042–1052.
- 14 Y.-M. Zhang, Y.-H. Liu, J. Zhang, Q. Liu, Z. Huang and X.-Q. Yu, *RSC Adv.*, 2014, **4**, 44261–44268.
- 15 Z. Huang, Y.-H. Liu, Y.-M. Zhang, J. Zhang, Q. Liu and X.-Q. Yu, *Org. Biomol. Chem.*, 2015, **13**, 620–630.
- 16 Q.-F. Zhang, W.-J. Yi, B. Wang, J. Zhang, L. Ren, Q.-M. Chen, L. Guo and X.-Q. Yu, *Biomaterials*, 2013, **34**, 5391–5401.
- 17 W.-J. Yi, X.-C. Yu, B. Wang, J. Zhang, Q.-Y. Yu, X.-D. Zhou and X.-Q. Yu, *Chem. Commun.*, 2014, **50**, 6454–6457.
- 18 Y.-H. Zhang, Y. Chen, Y.-M. Zhang, Y. Yang, J.-T. Chen and Y. Liu, *Sci. Rep.*, 2014, **4**, 7471.
- 19 Y.-H. Zhang, Y.-M. Zhang, Q.-H. Zhao and Y. Liu, *Sci. Rep.*, 2016, **6**, 22654.
- 20 H. Liu, H. Wang, W. Yang and Y. Cheng, *J. Am. Chem. Soc.*, 2012, **134**, 17680–17687.
- 21 M. Wang, H. Liu, L. Li and Y. Cheng, *Nat. Commun.*, 2014, **5**, 3053–3060.
- 22 V. Gopal, *J. Controlled Release*, 2013, **167**, 323–332.
- 23 B. Wang, W.-J. Yi, J. Zhang, Q.-F. Zhang, M.-M. Xun and X.-Q. Yu, *Bioorg. Med. Chem. Lett.*, 2014, **24**, 1771–1775.
- 24 N. Jain, Y. Arntz, V. Goldschmidt, G. Duportail, Y. Mély and A. S. Klymchenko, *Bioconjugate Chem.*, 2010, **21**, 2110–2118.
- 25 M. Brunelle, A. Polidori, S. Denoyelle, A.-S. Fabiano, P. Y. Vuillaume, S. Laurent-Lewandowski and B. Pucci, *C. R. Chim.*, 2009, **12**, 188–208.
- 26 J.-H. Fuhrhop and T. Wang, *Chem. Rev.*, 2004, **104**, 2901–2938.
- 27 L. Latxague, M. A. Ramin, A. Appavoo, P. Berto, M. Maisani, C. Ehret, O. Chassande and P. Barthélémy, *Angew. Chem., Int. Ed.*, 2015, **54**, 4517–4521.
- 28 N. Jain, V. Goldschmidt, S. Oncul, Y. Arntz, G. Duportail, Y. Mély and A. S. Klymchenko, *Int. J. Pharm.*, 2012, **423**, 392–400.
- 29 S. Grinberg, V. Kolot, C. Linder, E. Shaubi, V. Kas'yanov, R. J. Deckelbaum and E. Heldman, *Chem. Phys. Lipids*, 2008, **153**, 85–97.
- 30 G. R. Dakwar, I. A. Hammad, M. Popov, C. Linder, S. Grinberg, E. Heldman and D. Stepensky, *J. Controlled Release*, 2012, **160**, 315–321.
- 31 S. Denoyelle, A. Polidori, M. Brunelle, P. Y. Vuillaume, S. Laurent, Y. ElAzhary and B. Pucci, *New J. Chem.*, 2006, **30**, 315–321.
- 32 I. Koltover, T. Salditt, J. O. Rädler and C. R. Safinya, *Science*, 1998, **281**, 78–81.
- 33 M. A. W. Eaton, T. S. Baker, C. F. Catterall, K. Crook, G. S. Macaulay, B. Mason, T. J. Norman, D. Parker, J. J. B. Perry, R. J. Taylor, A. Turner and A. N. Weir, *Angew. Chem., Int. Ed.*, 2000, **112**, 4229–4233.
- 34 G. G. M. D'Souza, R. Rammohan, S.-M. Cheng, V. P. Torchilin and V. Weissig, *J. Controlled Release*, 2003, **92**, 189–197.
- 35 G. G. M. D'Souza, S. V. Boddapati and V. Weissig, *Mitochondrion*, 2005, **5**, 352–358.
- 36 J. Gaucheron, C. Santaella and P. Vierling, *Bioconjugate Chem.*, 2001, **12**, 569–575.
- 37 K. Fabio, J. Gaucheron, C. Di Giorgio and P. Vierling, *Bioconjugate Chem.*, 2003, **14**, 358–367.
- 38 G. Zuber, L. Zammuto-Italiano, E. Dauty and J.-P. Behr, *Angew. Chem., Int. Ed.*, 2003, **42**, 2666–2669.
- 39 C. Lainé, E. Mornet, L. Lemiègre, T. Montier, S. Cammas-Marion, C. Neveu, N. Carmoy, P. Lehn and T. Benvegna, *Chem. – Eur. J.*, 2008, **14**, 8330–8340.
- 40 J.-X. Chen, X.-D. Xu, S. Yang, J. Yang, R.-X. Zhuo and X.-Z. Zhang, *Macromol. Biosci.*, 2013, **13**, 84–92.
- 41 D. Y. Cho, H. Cho, K. Kwon, M. Yu, E. Lee, K. M. Huh, D. H. Lee and H. C. Kang, *Adv. Funct. Mater.*, 2015, **25**, 5479–5491.
- 42 K. Gupta, K. A. Afonin, M. Viard, V. Herrero, W. Kasprzak, I. Kagiampakis, T. Kim, A. Y. Koyfman, A. Puri, M. Stepler, A. Sappe, V. N. KewalRamani, S. Grinberg, C. Linder, E. Heldman, R. Blumenthal and B. A. Shapiro, *J. Controlled Release*, 2015, **213**, 142–151.
- 43 Q. Liu, Q.-Q. Jiang, W.-J. Yi, J. Zhang, X.-C. Zhang, M.-B. Wu, Y.-M. Zhang, W. Zhu and X.-Q. Yu, *Bioorg. Med. Chem.*, 2013, **21**, 3105–3113.
- 44 W.-J. Yi, Q.-F. Zhang, J. Zhang, Q. Liu, L. Ren, Q.-M. Chen, L. Guo and X.-Q. Yu, *Acta Biomater.*, 2014, **10**, 1412–1422.
- 45 H. Zeng, M. E. Johnson, N. J. Oldenhuis, T. N. Tiambeng and Z. Guan, *ACS Cent. Sci.*, 2015, **1**, 303–312.
- 46 W.-X. Wu, N. Wang, B.-Y. Liu, Q.-F. Deng and X.-Q. Yu, *Soft Matter*, 2014, **10**, 1199–1213.
- 47 D. Lleres, E. Dauty, J.-P. Behr, Y. Mély and G. Duportail, *Chem. Phys. Lipids*, 2001, **111**, 59–71.
- 48 Y. Liu and T. M. Reineke, *J. Am. Chem. Soc.*, 2005, **127**, 3004–3015.
- 49 M. Ma, F. Li, Z.-F. Yuan and R.-X. Zhuo, *Acta Biomater.*, 2010, **6**, 2658–2665.
- 50 T. Kim, K. A. Afonin, M. Viard, A. Y. Koyfman, S. Sparks, E. Heldman, S. Grinberg, C. Linder, R. P. Blumenthal and B. A. Shapiro, *Mol. Ther. – Nucleic Acids*, 2013, **2**, e80.
- 51 Q.-F. Zhang, Q.-Y. Yu, Y. Geng, J. Zhang, W.-X. Wu, G. Wang, Z. Gu and X.-Q. Yu, *ACS Appl. Mater. Interfaces*, 2014, **6**, 15733–15742.